Conduction mechanism in ultrathin metallic films

O. Pfennigstorf, A. Petkova, H. L. Guenter, and M. Henzler*
Institut für Festkörperphysik, Universität Hannover, Appelstrasse 2, D-30167 Hannover, Germany
(Received 22 August 2001; published 3 January 2002; published 3 January 2002)

The conduction mechanism in ultrathin films may differ from bulk materials due to different effects: surface scattering and quantum size effect should be considered. Also weak localization and superconductivity may be important. All those effects are detected with the magnetoconductance. Therefore epitaxial Pb films have been grown on Si(111) 7×7 in ultrahigh vacuum at low temperatures. With conductance and magnetoconductance *in situ* those contributions are separated. Due to detailed structural informations from spot profile analysis of low-energy electron diffraction the effect of film disorder and surface roughness is revealed for all scattering processes.

DOI: 10.1103/PhysRevB.65.045412 PACS number(s): 73.50.Jt, 73.61.At, 68.55.Jk, 61.14.Hg

I. INTRODUCTION

Ultrathin metal films with a thickness of one or a few monolayers draw more and more interest, since they are now available as epitaxial films on insulating substrate and are therefore the best model systems for two-dimensional (2D) conduction in metal systems. Additionally semiconductor technology requires thinner and thinner films, so that the properties due to restriction to thicknesses of a few monolayers get also technological importance. Since the detailed atomic structure and the restriction to a thickness smaller than the bulk mean free path may modify the transport mechanism dramatically, the atomic structure and the electronic transport properties have to be measured on the same films.

For the production of a film as perfect as possible the substrate should be perfect. Therefore the Si(111) 7×7 surface has been selected, since it may be produced with large step free areas. For a simple structure of the metal film chemical reaction with the substrate has to be avoided. Therefore only metals, which do not form silicides, such as Ag, Pb, or In, are suited for a fundamental study. Experiments with epitaxial Ag films have shown, that for ultrathin films weak localization and a metal insulator transition dominate the transport mechanism at low temperatures.[1,2] The diffusion of Ag at low temperatures is not very high, so that the formation of well ordered films at low temperatures is difficult. On the other hand Pb shows high mobility and forms readily dense monolayers on silicon.[3] The growth even at low T is layer-by-layer.[4–9] Additionally the superconductivity might give more information on the conduction mechanism. Therefore epitaxial films of Pb have been produced on Si(111) 7×7 at low temperatures. The structure and the defects of the films have been studied carefully with spot profile analysis of low energy electron diffraction (SPA-LEED).[8,9]

The classic model for description of the conduction mechanisms in metals is the so called Drude model. It is assumed, that the electrons have a mean free path, until by a scattering process the additional velocity gained in an external electric field is randomized. A perfect crystal should yield an infinite free path. All defects like point defects (vacancies, interstitials, and foreign atoms), line defects such as dislocations, plane defects such as grain boundaries, and thermal vibrations contribute to scattering. For thin films additionally surface scattering and interference (weak localization and quantization) have to be considered. Superconductivity is a bulk phenomenon, it may change due to film thickness and structure. For thin films additionally the superconducting fluctuations have to be considered.[10,11] Therefore the conductance of the Pb films, fully characterized with respect to structure and defects during and after growth and annealing, has been measured *in situ* at temperatures between 4 and 300 K. Results with conductivity measurements are in the literature.[4–6,12,13] The conductivity provides a first information. Measurements of the Hall effect show the changes of the band structure with film thickness.[7] New Hall effect measurements together with calculations of the band structure will be published soon. Magnetoconductance results are presented here, since they are the best tool to identify the scattering mechanisms.

II. EXPERIMENTAL SETUP

For production of perfect epitaxial films Si(111) surfaces in size of 15×15 mm^2 have been prepared in ultrahigh vacuum by annealing and flashing up to 1500 K of chemically oxidized samples. Using well oriented samples and a proper cooling cycle provided fairly step free surfaces, as checked with spot profile analysis of LEED (SPA-LEED).[8,9,14] With a He cryostat the sample could be cooled to 15 K during deposition of Pb and, after closing of the cooled shutter, to 4 K for measurement. For the electric measurements the samples had four predeposited Mo contacts in the corner for a van der Pauw measurement.[15] The temperature has been measured with a Pt(100) and a Si diode at the bottom of the cryostat, which has been calibrated against a Si diode glued on a dummy Si sample in measuring position. The superconductivity of bulk Pb provided a perfect check. Within uhv and at low temperatures the sample could be shifted into a split coil magnet of 4 Ts for measurement of the magnetoconductance (Fig. 1).

The films have been deposited at about 15 K. The conductance could be measured simultaneously. For magnetoconductance the deposition has been interrupted, the shutter has been closed and the sample shifted into the supercon-

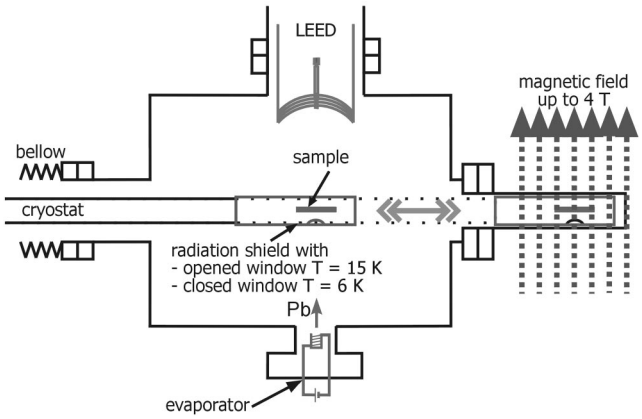

FIG. 1. Experimental setup for production and measurement of ultrathin Pb films on Si(111) 7×7 at low temperatures.

ducting magnet. The structure of the film has been sometimes checked *in situ* before or after the electrical measurements. Most LEED investigations have been done in a separate uhv system reproducing the production parameters.[8,9]

III. RESULTS

A. Annealed films

The measurement of the conductance during deposition of Pb onto Si(111) 7×7 at 15 K has shown, that the conduction mechanisms changes with film thickness. This change is connected with structural changes, as shown in Fig. 2.[13]

The lower slope of conductance up to 4.5 ML is obviously connected with the disorder in the growing film, as shown in the inset with LEED data. Since magnetoconductance was not possible to be measured during growth, the following

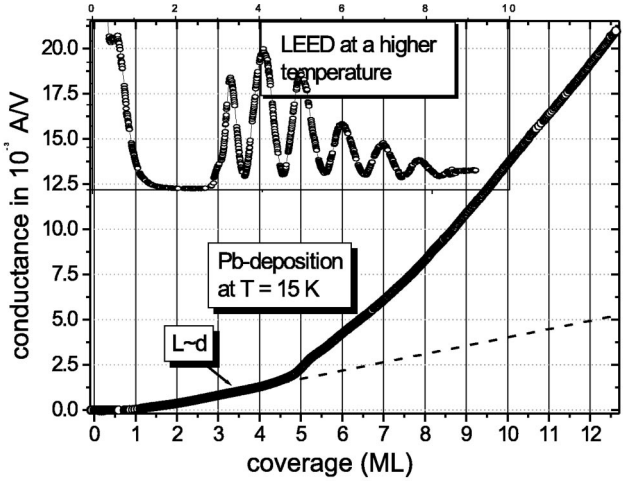

FIG. 2. Conductance of a Pb film during deposition onto insulating Si(111) 7×7 at 15 K. Up to 0.7 ML no conductance is observed. Up to 4.5 ML the linear increase points to bulk defect scattering. After recrystallization at about 5 ML the increase is steeper and more than linear. The inset shows the LEED intensity for deposition at higher temperatures, so that the recrystallization starts already at 3.5 ML (figure from Ref. 13).

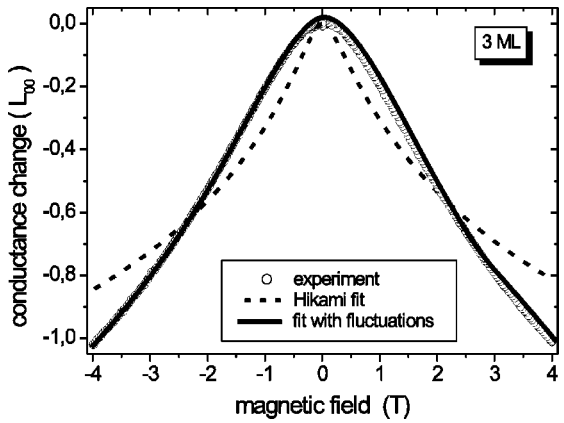

FIG. 3. Magnetoconductance of a Pb film (3 ML) at about 6.8 K. The best fit using only weak localization (dashed line) is called Hikami fit, a perfect fit (solid line) is only obtained by inclusion of superconducting fluctuations. Here the conductance quantum $L_{00}=2e^2/h=0.7810^{-4}\ A/V$ has been used for the ordinate.

data have been recorded after interruption of deposition. For clarifying the conductance mechanisms annealed films have been studied at 7 K (if not indicated otherwise) and roughness has been added by deposition onto annealed films, to separate different contributions to the conduction mechanism. Due to the lower temperature (after closing the shutter) the superconducting contributions could be more clearly identified. As seen in the former studies with Ag films[1,2] in addition to thermal and roughness scattering weak localization has been expected as the dominant scattering mechanism. The fitting, however, has been completely unsatisfying (Fig. 3). In addition to an unreasonably high contribution of antilocalization no acceptable fit was possible. As soon as the superconduction fluctuations[10,11] are included, using the theories of Aslamov-Larkin[16] and Maki-Thompson,[17,18] a perfect fit is possible (Fig. 3). The correction of the conductance due to superconducting fluctuations is given by Aslamov and Larkin[16] as

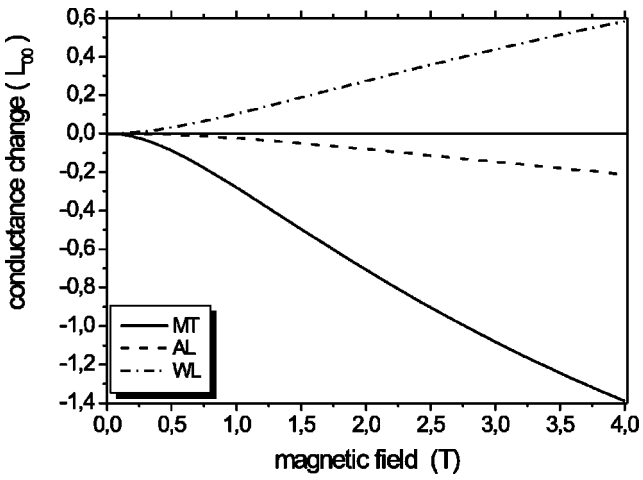

FIG. 4. Contributions of weak localization (WL) and of superconducting fluctuations according to Maki-Thompson (MT) and Aslamov-Larkin (AL) to the magnetoconductance as shown in Fig. 2.

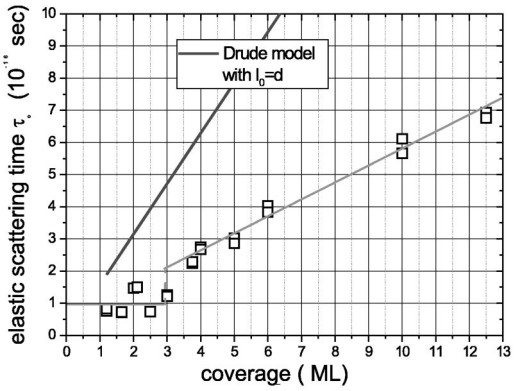

FIG. 5. Elastic scattering times τ_0 for annealed Pb films on Si(111) 7×7 at about 7 K. For the calculation with the Drude model (upper solid line) the mean free path l_0 is set equal to the film thickness d.

$$\Delta_{\mathrm{AL}}(B)=L_{00}\pi^2/4\ln(T/T_C)\{2B_4/B-(2B_4/B)^2[\Psi(1+B_4/B)-\Psi(1/2+B_4/B)]-1/2\}. \quad (1)$$

B_4 is calculated from

$$B_4=2k_BT\ln(T/T_C)/\pi eD. \quad (2)$$

B_4 is the field corresponding to the superconducting fluctuations and k_B is Boltzmann's constant. The second correction due to superconduction fluctuations is due to the theory of Maki and Thompson[17,18]

$$\Delta_{\mathrm{MT}}(B)=L_{00}\pi^2/4\ln(T/T_C)B_4/(B_4-B_3)\times[f(B_4/B)-f(B_3/B)]. \quad (3)$$

B_3 is taken from the theory of weak localization, it contains inelastic and magnetic scattering. The temperature dependence has been calculated by Ebisawa *et al.*[27]

$$\Delta L_{\mathrm{MT}}=L_{00}=\pi^2/4\ln(T/T_C)-\delta\ln[\ln(T/T_C)/\delta] \quad (4)$$

with the pair breaking parameter δ

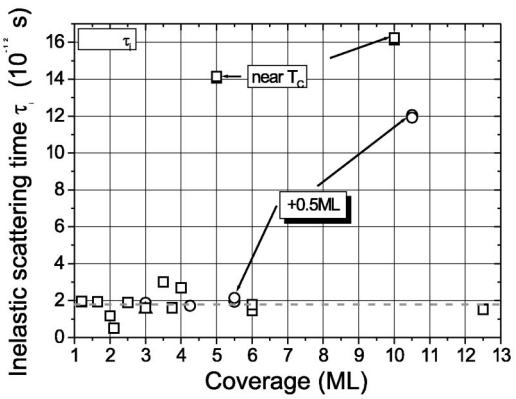

FIG. 6. Inelastic scattering times τ_i for annealed Pb films on Si(111) 7×7 at about 7 K. For films close to the superconducting transition temperature the fitting procedure obviously did not work properly.

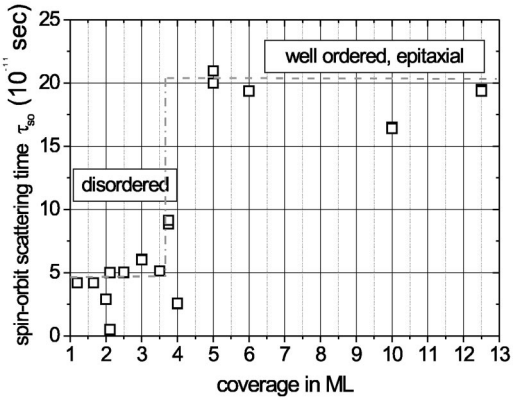

FIG. 7. Spin-orbit scattering times τ_{SO} for annealed Pb films on Si(111) 7×7.

$$\delta=\pi\hbar/8k_BT\tau_i. \quad (5)$$

The fluctuations yield a correction to the conductance, using both the theories of Aslamov and Larkin and of Maki and Thompson. The fit using both weak localization and superconducting fluctuations provides all essential scattering parameters τ_0, τ_i, τ_{SO}, and T_C.

The fit provides due to its high precision detailed informations on the relevant scattering parameters as elastic scattering time τ_0, inelastic scattering time τ_i, spin-orbit scattering time τ_{SO}, superconducting transition temperature T_c, even when that temperature is lower than the temperature of measurement, and the contributions of weak localization and superconducting fluctuations to the actual conductance. Those contributions are shown separately in Fig. 4.

The contributions of superconducting fluctuations are the larger, the closer the temperature is to the transition temperature of superconductivity as seen, for example, in Fig. 9. The magnetoconductance has been measured for many film thicknesses after annealing up to the temperature of highest conductance (150 to 300 K depending on film thickness). After overheating the conductance decreases again due to island formation. The following figures show the scattering times and the transition temperatures for well annealed films.

In Fig. 5 the elastic scattering times τ_0 are shown. For disordered films (up to 3 ML) a constant and very low scat-

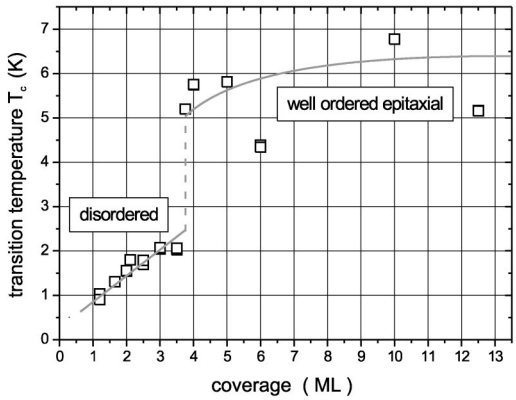

FIG. 8. Transition temperature T_c for superconductivity for Pb films on Si(111) 7×7.

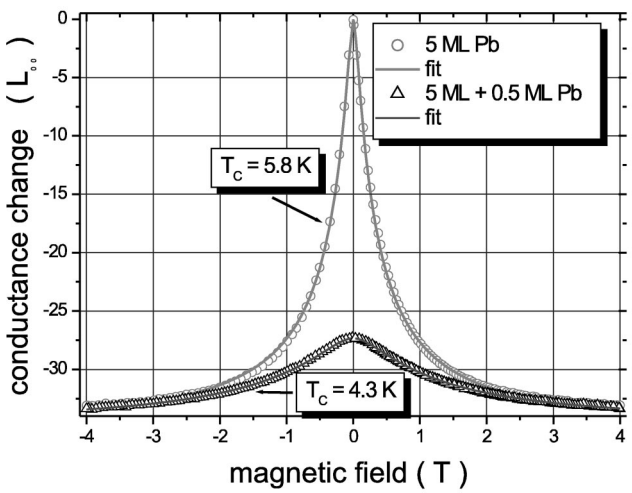

FIG. 9. Magnetoconductance of a Pb film (5 ML) after annealing and after additional deposition of 0.5 ML at 15 K. Measurement at about 7 K. The curves are plotted to coincide at maximum magnetic field.

tering time is found. It points to a constant bulk mobility, so that surface scattering is not important. The films with $d > 4$ ML are epitaxial and show a scattering time proportional to thickness. Therefore surface and/or interface scattering should be the dominant effect. Since the surface scattering is increased by additional deposition at low temperature (see the following section), the surface should be specular and the scattering due to the interface is most important. If a simple Drude model is used, the mean free path is only one third of the thickness. Therefore the scattering of the interface cannot be described by a simple diffuse scattering of the interface.

The inelastic scattering times τ_i (Fig. 6) are nearly independent of thickness. For some films the measuring temperature was close to the transition temperature T_c, so that fitting was possible only by applying a small magnetic field to suppress superconductivity. In those cases the fitting procedure obviously has been not accurate.

The spin-orbit scattering time τ_{SO} (Fig. 7) again depends on the structure: the disordered films show a much lower time than the ordered epitaxial films. Finally the transition temperatures T_c are shown (Fig. 8). Remarkedly temperatures down to 1 K are evaluated, although all measurements have been performed close to 7 K. Surprisingly the transition temperature increases proportional to thickness for the disordered films. For the ordered films values close to the bulk value have been found.

B. Rough films

To study the influence of roughness in detail, annealed films have been used to deposit at low-temperature half a monolayer, so that with LEED the additional roughness (half of the step height) and the correlation length (given by island distance) are completely characterized. As an example the magnetoconductance of an annealed film with 5 ML is shown together with the results of the same film after deposition of an additional half monolayer (Fig. 9). For easy comparison the curves are plotted to fit at maximum field, where due to negligible superconducting contributions a coincidence is a good approximation.

Table I shows that both the elastic scattering time and the critical temperature T_c are remarkedly reduced by the roughness, although the average thickness is increased.

C. Dependence on temperature

For some samples the magnetoconductance has been measured for temperatures between 3 and 40 K (the lowest temperatures have been produced by pumping of the liquid He). Here the conductances at zero and maximum field are shown, since a sufficient stabilization of an arbitrary temperature over the full time of a scan of the magnetic field is difficult. Therefore only scans with constant magnetic field are shown. For an annealed film with 3 ML first a decrease and then an increase is seen with increasing temperature. For the measurement with magnetic field a steady increase with temperature points to the localization of the carriers in the ultrathin film (Fig. 10).

For thicker films ($d > 4$ ML) the conductance decreases in the full temperature range, so that only superconducting fluctuations for low magnetic fields and defect and thermal scattering for all magnetic fields are important (Fig. 11).

An evaluation of the fits of the differences in Figs. 10 and 11 provides the temperature dependence of the inelastic scattering time τ_i. The power for the higher temperatures depends strongly on the structure of the film (Fig. 12).

TABLE I. Changes of elastic scattering time τ_0 and transition temperature T_c due to deposition of 0.5 ML at low temperatures onto well annealed Pb films.

Film thickness after anneal (ML)	Thickness after adding 0.5 ML	Elastic scattering time τ_0 (10^{-16} sec)		Superconducting transition T_c (K)	
2.5		0.8		1.8	
	3		0.7		2
3.75		2.2		5.2	
	4.25		2.1		4.9
5		3.0		5.8	
	5.5		2.5		4.3
10		6.0		6.8	4.3
	10.5		4.0		6.7

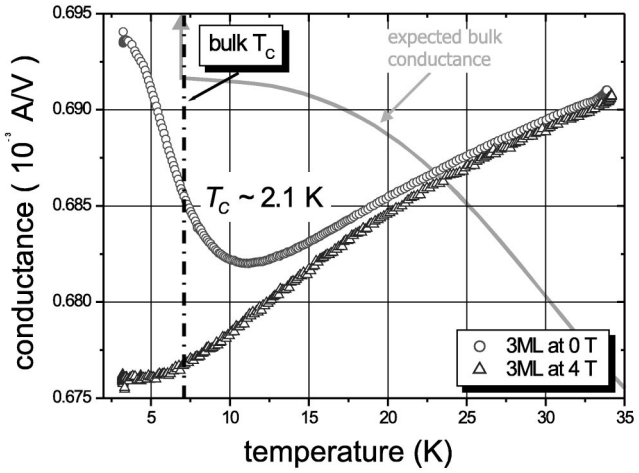

FIG. 10. Conductance vs temperature for a Pb film (3 ML) without and with magnetic field (4 T), respectively. The superconducting fluctuations are suppressed by the magnetic field.

D. Films on annealed monolayer

Epitaxial films of especially high perfection have been produced by deposition of a bit more than a monolayer at 15 K and annealing to room temperature. Here a well ordered monolayer is produced with the residual Pb forming perfect epitaxial islands. Further deposition at low temperatures produces epitaxial films, where the small rotation of grains in the mosaic structure is further reduced and the grain size increased.[8,9] It has been tested, to what extent the scattering parameters are modified. Here even films with a total thickness of less than 4 ML are epitaxial and they show higher perfection than epitaxial films with higher thickness deposited directly onto Si(111) 7×7. Here the results of a film with total thickness of 2.75 monolayers (by deposition onto an annealed monolayer with islands) are shown in more detail (Fig. 13).

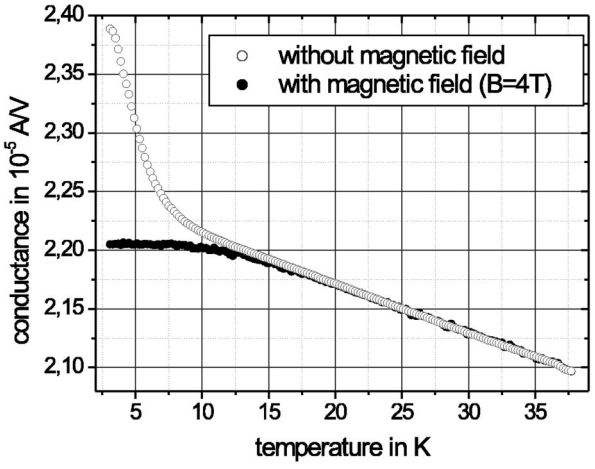

FIG. 11. Conductance vs temperature for a Pb film (4 ML) without and with magnetic field (4 T), respectively. The well ordered film shows the classical increase of resistance with temperature after suppression of the superconducting fluctuations due to the magnetic field.

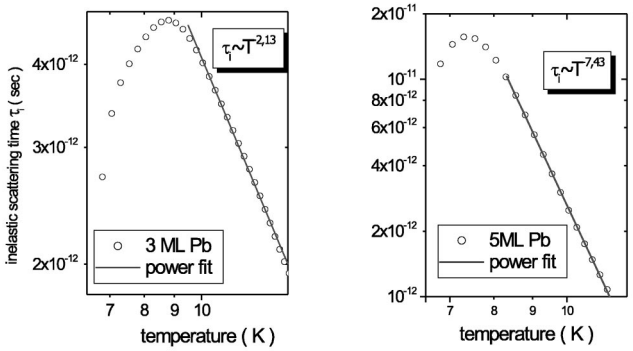

FIG. 12. Inelastic scattering time τ_i for a film with 3 ML (disordered) and with 5 ML (ordered) vs temperature.

The scattering times and the critical temperature are shown in Table II in comparison with a disordered film of the same thickness and an epitaxial film of 5 ML with more defects due to deposition onto 7×7. It is seen, that the perfect film has a much higher elastic scattering time than the other two films. Otherwise the perfect film agrees well with the other epitaxial film.

IV. DISCUSSION

A. Structure of films

For a discussion of the conduction mechanism in the Pb films both the structural and the electric results have to be used. The structural information from the SPA-LEED measurements[8,9] is summarized in the Fig. 14. The first monolayer grows even at 15 K in a rather ordered pseudomorphic structure, producing a modified 7×7 structure, where Pb and Si atoms probably are mixed in the top layer. The following layers grow at 15 K in a disordered arrangement due to the large misfit. For more than 4 monolayers thickness a recrystallization process with a Pb film with bulk

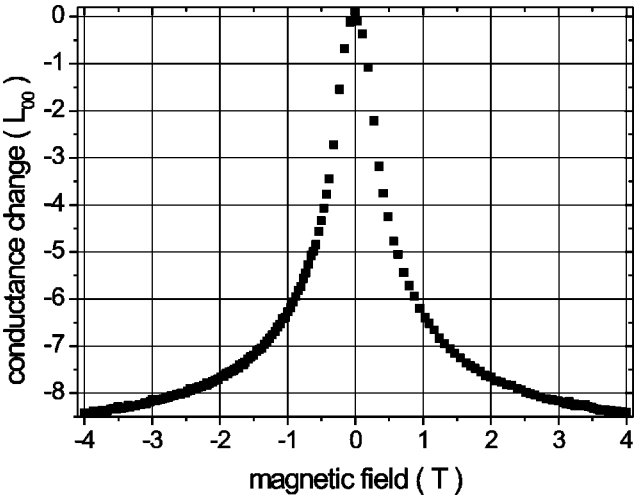

FIG. 13. Magnetoconductance of an ordered Pb film (2.75 ML) after annealing of a monolayer (300 K) and additional deposition of 1.75 ML at 15 K (temperature $T \approx 7$ K).

TABLE II. Comparison of an epitaxial film (2.75 ML), produced by deposition of 1.75 ML onto an annealed Pb monolayer at low T, with films deposited directly onto Si(111) 7×7: a disordered film of 3 ML and an epitaxial film (5 ML).

	Elastic scattering τ_0	Spin orbit τ_{SO}	Critical T_c
Epitaxial 2.75 ML (Including 1 ML annealed)	6×10^{-16} sec	2×10^{-10} sec	4.9 K
Disordered 3 ML	1×10^{-16} sec	0.5×10^{-10} sec	2 K
Epitaxial 5 ML on 7×7	3×10^{-16} sec	2×10^{-10} sec	5.8 K

lattice constant and [111] orientation starts, which reproduces the orientation of the substrate. Therefore at least part of the film recrystallizes down to the interface. Due to different starting points for crystallization the film shows stacking faults and a mosaic structure with small angle grain boundaries close to the perfect epitaxial orientation. If Pb is deposited onto an annealed monolayer with Pb islands, the recrystallization obviously starts at the Pb islands producing an epitaxial film with negligible mosaic misorientation and no disordered film between epitaxial film and substrate.

B. Annealed films

The simplest model would be to describe the system as a layering of three more or less independent layers with increasing conductivity. It describes with the first layer the percolation process and film growth up to the monolayer. The second layer from 1 to 4 ML is already well described with the extremely low and constant elastic scattering time τ_0 (Fig. 5). The higher conductivity of the epitaxial film asks for a larger elastic scattering time. The linear increase with thickness (Fig. 5) may be described either with interface scattering or with a dead layer at the interface with very small conductivity. Surface scattering can be ruled out for the annealed surfaces, since roughness scattering after deposition of half a monolayer onto the annealed surface at low temperatures is quantitatively described by starting with a mirror like surface.[13] Interface scattering works here similar to a dead layer with a thickness of 3 to 4 ML. A simple diffuse interface scattering (neglecting corrections due to superconducting fluctuations) yields a higher elastic scattering time than measured (Fig. 5).

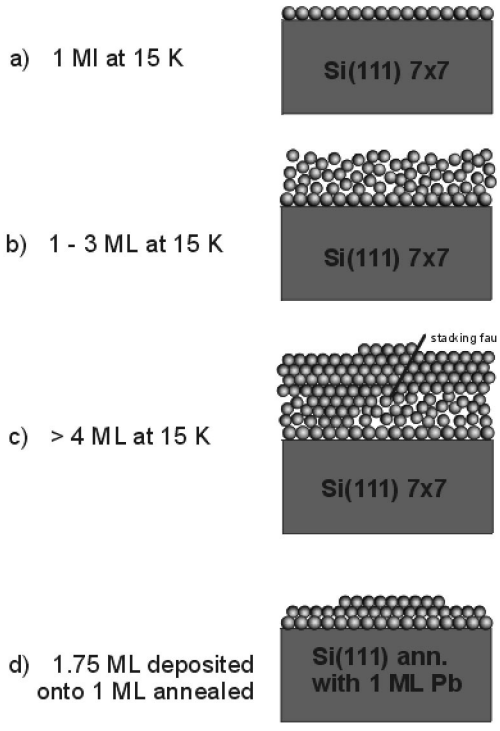

FIG. 14. Schematic structure of Pb films on Si(111) 7×7: (a) 1 ML Pb deposited at 15 K onto Si(111) 7×7 (pseudomorphic), (b) disordered film on pseudomorphic monolayer, (c) recrystallization as epitaxial films (lattice constant of bulk Pb) with grain boundaries due to a small mosaic rotational disorder and with stacking faults, (d) highly perfect film due to deposition onto an annealed monolayer (Refs. 8,9).

Therefore the corrections due to weak localization, quantum size effect and superconducting fluctuations are needed for a description of the conduction mechanism. The substantial increase due to superconducting fluctuations is seen in the Figs. 10 and 11. For films with a thickness of more than 4 ML the usual description with thermal scattering (resistance $R\propto T$ for high T) and residual resistance due to defect and surface scattering is sufficient only when corrections due to weak localization and superconducting fluctuations are included. With the magnetic field those corrections are essentially suppressed. The reduced elastic scattering time τ_0 in Fig. 5 corresponding to a mean free path of only a fraction of the layer thickness points to the inadequacy of the simple Drude model neglecting many corrections.

For films with a thickness of less than 4 ML the conductivity increases with increasing temperature (except in the regime of superconducting fluctuations), as shown in Fig. 10. A clear result for 1 ML has been presented in Ref. 12. As already seen with Ag films,[1,2] the increase is outside the range of weak localization, it is more adequately described by a strong localization. It should be noted, that this temperature dependence is not restricted to the disordered films. Also the ultrathin epitaxial film of Sec. IV shows the same temperature dependence as the disordered film of same average thickness. A model may use a change of the band structure with thickness. From LEED data it is known, that also the disordered films have a rather constant thickness. From Hall effect (to be published) it is evident, that the band structure depends essentially on average thickness, not on structure. The Hall voltage is identical for ordered and disordered films of the same thickness. Therefore a thickness dependence of band structure, e.g., Fermi surface or even the formation of a

gap, is a good candidate for description of the temperature dependence, unusual for a metal. Unfortunately a computation of band structure, which might provide the temperature dependence, is still missing.

Superconductance fluctuations cause substantial modifications, especially close to the transition temperature. Within the fitting calculations they have been especially helpful, since they provided exact values for the different scattering times and the superconduction transition temperature.

The variations of the elastic scattering have been already discussed, showing that the structural defects are the dominant factors. The disordered film shows the lowest values, so low that the ''mean free path'' using bulk fermi velocity is much lower than atomic distance. Therefore a simple meaning of this quantity is not available.

The inelastic scattering time at 7 K is independent of structure and film thickness (Fig. 6). The few values above the average are obviously due to fitting inaccuracies close to the superconducting transition, where the contributions due to fluctuations are large and the normal state (only the normal state may be used for the fitting procedure) is obtained only with a small magnetic field. The temperature dependence of the time τ_i shows for temperatures around 10 K a clear power dependence $\tau_i \propto T^{-P}$ (Fig. 12). For electron phonon scattering a power $P=2$ is expected.[11,10,19–21] For the film with 3 ML the experimental value is close to the prediction. For the film with 5 ML, however, no theory is known, which would fit to the high experimental value of $P=7.43$. For this film the linear temperature dependence of the resistance beyond 15 K has also been evaluated assuming that the resistance increase is just due to inelastic scattering (Matthiesen's rule). The value of τ_i, determined with the Drude equation, however, differs from the value from the fitting of the magnetoresistance by more than one order of magnitude. This difference may be due to the quantum size effect. Trivedi[22] pointed out, that Matthiesen's rule is no more valid in the regime of quantum size effect. As a result the quantum size effect may be important even at fairly high temperatures.

The spin-orbit scattering time τ_{SO} (Fig. 13) shows two different values, a low value for the disordered films and a high value for the epitaxial films. A correlation between elastic and spin-orbit scattering times has been reported in literature.[23–26] This correlation reflects the correlation between atomic arrangement and electronic structure. The increase of the elastic scattering time with thickness from 4 to 12 ML, however, is not reproduced by a change of the spin-orbit time.

C. Rough films

For a clear separation of the roughness contribution to the conduction mechanism well annealed films have been cooled down to 15 K and half a monolayer has been deposited. From LEED measurements it is known, that islands are formed with monolayer height. Therefore roughness and correlation length are known. The corresponding electrical measurements can therefore directly describe the influence of roughness, since the simultaneous thickness change is small. The conductance showed a clear decrease during deposition of the first half monolayer (see Fig. 2 in Ref. 13). From the present measurements it is clear, that the decrease is due to a combination of roughness, quantum size effect and superconducting fluctuations. The fitting provides with the elastic scattering time and with the transition temperature detailed informations, which have not yet been used for a theoretical and quantitative interpretation. Especially the direct correlation of roughness and superconducting transition looks worthwhile for a theoretical model.

V. CONCLUSION

For fundamental 2D measurements of metallic films it is necessary to produce structurally well defined ultrathin epitaxial films in ultrahigh vacuum at low temperatures and to characterize structural details quantitatively, as done here with SPA-LEED. With these prerequisites the combination of conductance and magetoconductance provides many details on the conduction mechanisms in ultrathin metallic films. Unfortunately the results may be described with available models only in part. It is hoped, that the results presented here may encourage theoreticians for providing models suited for quantitative description.

The presented results were obtained with substrates of high symmetry. Using higher index surfaces as substrates will result in asymmetric films and even 1D structures. Those experiments are in progress.

ACKNOWLEDGMENTS

We thank for helpful discussions with J. Wollschläger, I. Vilfan, H. Apel, and H.J. Everts. We gratefully acknowledge the support of the Deutsche Forschungsgemeinschaft.

*Author to whom correspondence should be addressed.

[1] M. Henzler, T. Lüer, and A. Burdach, Phys. Rev. B **58**, 10 046 (1998).
[2] M. Henzler, T. Lüer, and J. Heitmann, Phys. Rev. B **59**, 2383 (1999).
[3] V.G. Lifshits, A.A. Saranin, and A.V. Zotov, *Surface Phases on Silicon* (Wiley, New York, 1994).
[4] M. Jalochowski and E. Bauer, Phys. Rev. B **38**, 5272 (1988).
[5] M. Jalochowski, H. Knoppe, G. Lilienkamp, and E. Bauer, Phys. Rev. B **46**, 4693 (1992).
[6] M. Jalochowski, E. Bauer, H. Knoppe, and G. Lilienkamp, Phys. Rev. B **45**, 13 607 (1992).
[7] M. Jalochowski, M. Hoffmann, and E. Bauer, Phys. Rev. Lett. **76**, 4227 (1996).
[8] A. Petkova, J. Wollschläger, H.-L. Günter, and M. Henzler, Surf. Sci. **471**, 11 (2001).
[9] A. Petkova, J. Wollschläger, H.L. Günter, and M. Henzler, Surf. Sci. **482-485**, 922 (2001).
[10] G. Bergmann, Z. Phys. B: Condens. Matter **48**, 5 (1982).
[11] C. Roth, C. Sürgers, and H. v. Löhneysen, Phys. Rev. B **54**, 3454

(1996).
[12] O. Pfennigstorf, K. Lang, H.-L. Günter, and M. Henzler, Astron. Astrophys., Suppl. Ser. **162**, 537 (2000).
[13] O. Pfennigstorf, A. Petkova, Z. Kallassy, and M. Henzler (unpublished).
[14] M. Horn-von Hoegen, Z. Kristallogr. **214**, 1 (1999).
[15] L. J. van der Pauw, Philips Res. Rep. **13**, 1 (1958).
[16] L.G. Aslamov and A.I. Larkin, Phys. Lett. **26A**, 238 (1968).
[17] K. Maki, Prog. Theor. Phys. **40**, 193 (1968).
[18] R.S. Thompson, Phys. Rev. B **1**, 327 (1970).
[19] S. Heun, J. Bange, R. Schad, and M. Henzler, J. Phys.: Condens. Matter **5**, 2913 (1993).
[20] J.M. Gordon, C.J. Lobb, and M. Tinkham, Phys. Rev. B **28**, 4046 (1983).
[21] P. Santhanam and D.E. Prober, Phys. Rev. B **29**, 3733 (1984).
[22] N. Trivedi and N. W. Ashcroft, Phys. Rev. B **38**, 12 298 (1988).
[23] G. Bergmann, Z. Phys. B: Condens. Matter **48**, 5 (1982).
[24] G. Bergmann and C. Horriar-Esser, Phys. Rev. B **31**, 1161 (1985).
[25] C. van Haesendonk, M. Gijs, and Y. Bruynseraede, in *Springer Series in Solid State Sciences* (Springer, Berlin, 1985), Vol. 61, p. 221.
[26] R. Schad, S. Heun, T. Heidenblut, and M. Henzler, Phys. Rev. B **45**, 11 430 (1992).
[27] H. Ebisawa, S. Maekawa, and H. Fukuyama, Solid State Commun. **45**, 75 (1983).